Korean J. Chem. Eng., **31**(7), 1237-1245 (2014)
DOI: 10.1007/s11814-014-0030-6

pISSN: 0256-1115
eISSN: 1975-7220

Impact of speciation on CO_2 capture performance using blended absorbent containing ammonia, triethanolamine and 2-amino-2-methyl-1-propanol

Hao-Yang Song*, Soo-Bin Jeon*, Se-Yong Jang, Sang-Sup Lee***, Seong-Kuy Kang****, and Kwang-Joong Oh*,†**

*Department of Environmental Engineering, Pusan National University, San 30, Jangjeon-dong, Busan 609-735, Korea
**Facility Division, Pusan National University, San 30, Jangjeon-dong, Busan 609-735, Korea
***Department of Environmental Engineering, Chungbuk National University,
52 Naesudong-ro, Heungdeok-gu, Cheongju 361-763, Korea
****Department of Environmental R&D, BK Environmental Construction, Songjuk-dong, Jangan-gu, Suwon 440-803, Korea
(*Received 7 October 2013 • accepted 23 January 2014*)

Abstract−In our previous study, a high CO_2 absorption rate was achieved using a blended absorbent containing AMP, NH_3, and TEA. The species of the blended absorbent was determined in this study using ^{13}C nuclear magnetic resonance (NMR) spectroscopy and a modified Kent-Eisenberg model. The carbamate formation constant was also regressed using the model. Bicarbonate and carbonate ions decrease the absorption efficiency and have a positive effect on CO_2 stripping. Carbamate has a negative effect on regeneration; a regeneration temperature of 373 K minimized the energy needed. In conclusion, the prediction equation and NMR analysis provide an easy way of determining carbonate group species and carbamate species concentrations, and this method will be helpful in optimizing CO_2 capture with blended absorbents.

Keywords: Blended Absorbents, Modified Kent-Eisenberg Model, Speciation, NMR, Absorption and Regeneration Efficiency

INTRODUCTION

The use of alkanolamines has been investigated as a possible technique for reducing CO_2 emissions from flue gases. Among various chemical absorbents, the sterically hindered amine AMP has higher absorption capacity and absorption rate and requires less regeneration energy than other amines [1-3]. The addition of ammonia (NH_3) has been proven to increase the CO_2 absorption rate and increase the CO_2 removal efficiency [1]. To reduce the loss of NH_3 vapor, various additives including amine and hydroxyl groups have been used, with vaporization having been extensively studied [4-6]. Studies using TEA to minimize the loss of NH_3 have been performed and the optimum blending ratio of AMP/NH_3/TEA was found to be 20/5/5 wt% [6]. It has been proven that blended amines have higher CO_2 absorption capacities and absorption rates than single amines (AMP and MEA). However, use of an AMP/NH_3/TEA blend in continuous absorption/desorption systems has not yet been investigated.

There are several factors affecting the absorption efficiency: the physical properties of the solvent, CO_2 partial pressure, absorption concentration, liquid temperature, and CO_2 loading of the solvent [7]. Ion speciation also has a significant effect on the regeneration and absorption efficiencies [8,9]. A previous study suggested that regeneration of CO_2 mainly originates from bicarbonate and carbonate species, and carbamate has a negative effect [10]. It is therefore necessary to investigate the ion species generated in amine/H_2O/CO_2 systems. The investigation of ion distribution can also improve our understanding of the reaction mechanism; it can also identify the effect of chemical structure on the CO_2 capture capacity, and of the operating conditions on species behaviors [11]. NMR spectroscopy is a tool that enables direct identification of carbon-containing compounds formed in CO_2 absorption and desorption processes [11-13]. By speciating CO_2/H_2O/amine, it is possible to reveal the relationships between stable carbamate formation and amine structure [14] and to identify the reaction mechanism [15]. Speciation can also verify thermodynamic models [14,16-18] and find the influence of reaction conditions on amine capacities for CO_2 capture [19]. However, there have been only a few studies on ion distribution in mixed amines. Ballard et al. showed the relative amounts of carbamate, bicarbonate, and other species as a function of time [20]. Francesco et al. used NMR analysis to study the CO_2 capture the performance of AMP-blended solvents, and showed that AMP-MDEA blends perform better than AMP-DEA due to the carbamate formation of DEA [21]. This shows that the ion species distribution affects CO_2 removal and desorption efficiencies. Hook et al. used NMR spectroscopy to quantify carbon containing ions and found that substituents in alpha position to the nitrogen increased absorption capacities and reduced the overall absorption rate. However, as the degree of substitution increased, the proportion of carbamate remaining in the equilibrated desorbed solution decreased [22].

To better understand species in CO_2/H_2O/mixed amine systems, the VLE data for CO_2 partial pressures and loadings were used in thermodynamic models. The electrolyte-NRTL model was based on the excess Gibbs energy to account for the electrostatic force due to the presence of ions in solution. In NRTL model [23], the

†To whom correspondence should be addressed.
E-mail: kjoh@pusan.ac.kr

long and short range interaction between the different species should be considered in the solution. The Deshmukh and Mather model is simpler and used the Guggenheim equation to represent activity coefficients [24]. The Kent-Eisenberg model is thermodynamically sound and reasonably simple compared to other models [25]. Models based on the Kent-Eisenberg equations have been widely used because of their simplicity and reasonable prediction power beyond the range of experimental data [26]. Tontlwachwuthlkul et al. [27] measured the solubility of CO_2 in AMP at various temperatures and AMP concentrations. They also correlated the data with a modified Kent-Eisenberg model and reported equations to determine equilibrium constants of the protonation reaction.

The objective of this study is to speciate blended amines containing AMP, NH_3, and TEA in CO_2 absorption and regeneration processes. The equilibrium among CO_2, the blended absorbent, and H_2O was investigated quantitatively using ^{13}C NMR spectroscopy. The Kent-Eisenberg model was used to predict species in the CO_2/H_2O/blended absorbent system; new correlations of the equilibrium constants of carbamate formation with temperature and CO_2 loading ratio are also presented. The measured and predicted species in the CO_2 capture process were compared. Based on the values obtained from continuous absorption and regeneration experiments, the CO_2 loading ratio, absorption and regeneration efficiencies, and speciation were investigated. This work will improve our understanding of the behavior of chemical species in CO_2 capture.

REACTION MECHANISM

1. Absorption Reaction Mechanism

In this study, the absorbent was formed by blending AMP, NH_3, and TEA in a fixed weight ratio of 20 : 5 : 5 wt%. The chemical reactions between CO_2 and the blended absorbent can be expressed by the following equations, where RNH_2 and R_3N represent AMP and TEA, respectively [17,18,28]. The main species formed in the studies systems are amine, protonated amine, amine carbamate, bicarbonate, carbonate, H_2O, H^+ and OH^-. The following chemical reactions are considered to take place in the liquid phase:

Dissociation of amines:

$$RNH_3^+ \overset{K_1}{\longleftrightarrow} RNH_2 + H^+ \quad (1)$$

$$H_2O + NH_3 \overset{K_2}{\longleftrightarrow} NH_4^+ + OH^- \quad (2)$$

$$R_3NH^+ \overset{K_3}{\longleftrightarrow} R_3N + H^+ \quad (3)$$

Formation of bicarbonate, carbamate:

$$H_2O + RNHCOO^- \overset{K_4}{\longleftrightarrow} HCO_3^- + RNH_2 \quad (4)$$

$$HCO_3^- + NH_3 \overset{K_5}{\longleftrightarrow} H_2O + NH_2COO^- \quad (5)$$

$$CO_2 + H_2O \overset{K_6}{\longleftrightarrow} HCO_3^- + H^+ \quad (6)$$

Auto-protolysis of water:

$$H_2O \overset{K_7}{\longleftrightarrow} H^+ + OH^- \quad (7)$$

Formation of carbonate:

$$HCO_3^- \overset{K_8}{\longleftrightarrow} CO_3^{2-} + H^+ \quad (8)$$

Note that the carbamate ion is formed only by the reaction of CO_2 with AMP and NH_3, not by CO_2 with TEA [29]. In the case of a hindered amine such as AMP, the carbamate is unstable [1,30], and decomposes to bicarbonate ion.

2. Speciation Prediction

We used the Kent-Eisenberg model to predict the species in the blended absorbent/H_2O/CO_2 system [27-29]. CO_2 pressure can be expressed as a function of the H^+ ion concentration and other known parameters such as equilibrium constants shown in Table 1, Henry's constant, initial absorbent concentration, CO_2 loading ratios. The CO_2 pressure can be calculated by determined H^+ ion concentration. The concentration of each species can be calculated using the equilibrium constants and the species balances. The Henry's low, which relates the CO_2 partial pressure to the concentration of physi-

Table 1. Equilibrium constants and Henry's law constant used in this work

Expression	Relation	Source
$K_1=\frac{m_{H^+}\, m_{RNH_2}}{m_{RNH_3^+}}$	$pK_1=14.933-1.8137\times10^{-2}T-1.6717m_{CO_2}+6.9818\times10^{2}m_{AMP}$	[31]
$K_2=\frac{m_{OH^-}\, m_{NH_3}}{m_{NH_4^+}}$	$\ln K_2=97.97152-\frac{5914.082}{T}-15.06399\ln T-1.100801*10^{-2}T$	[32]
$K_3=\frac{m_{H^+}\, m_{R_3N}}{m_{R_3NH^+}}$	$\ln K_3=97.51-\frac{9148.22}{T}-173.54\alpha m_{TEA}^{total}+31.28(\alpha m_{TEA}^{total})^{0.5}-14.82\ln T-0.0058T$	[34]
$K_4=\frac{m_{RNH_2}\, m_{HCO_3^-}}{m_{RNHCOO^-}}$	$\ln(1/K_4)=-4232.0399+37.6738\times\frac{10^5}{T}-111.8351\times\frac{10^7}{T^2}+110.7526\times\frac{10^9}{T^3}$	[35]
$K_5=\frac{m_{NH_2COO^-}}{m_{NH_3}\, m_{HCO_3^-}}$	$\ln K_5=20.15214-\frac{604.1164}{T}-4.017263\ln T-0.503095*10^{-2}T-2.27516\alpha+3.34403\alpha^2$	[32] and regress
$K_6=\frac{m_{H^+}\, m_{HCO_3^-}}{m_{CO_2}}$	$\ln K_6=-241.818+298.253\times\frac{10^3}{T}-148.528\times\frac{10^6}{T^2}+332.648\times\frac{10^8}{T^3}-282.394\times\frac{10^{10}}{T^4}$	[36]
$K_7=m_{H^+}\, m_{OH^-}$	$\ln K_7=39.5554-987.9\times\frac{10^2}{T}+568.828\times\frac{10^5}{T^2}-146.451\times\frac{10^8}{T^3}+136.146\times\frac{10^{10}}{T^4}$	[36]
$K_8=\frac{m_{H^+}\, m_{CO_3^{2-}}}{m_{HCO_3^-}}$	$\ln K_8=-297.74+364.385\times\frac{10^3}{T}-184.158\times\frac{10^6}{T^2}+415.793\times\frac{10^8}{T^3}-354.291\times\frac{10^{10}}{T^4}$	[36]
$P_{CO_2}=H_{CO_2}*m_{CO_2}$	$H_{CO_2}=1000\times\exp\left(192.876-\frac{9624.4}{T}-28.749\ln T+0.01441T\right)$	[37]

cally dissolved CO_2 in the solvent, is given as

$$P_{CO_2} = H_{CO_2} \times m_{CO_2} \quad (9)$$

where P_{CO_2} is the partial pressure of CO_2 (kPa) and H_{CO_2} is the Henry's law constant.

In addition to the equation defining the equilibrium constants, additional equations describing the amine balance, total carbon balance, and ion charge balance of the system can be written as

$$m^{total}_{RNH_2} = m_{RNH_2} + m_{RNH_3^+} + m_{RNHCOO^-} \quad (10)$$

$$m^{total}_{NH_3} = m_{NH_3} + m_{NH_4^+} + m_{NH_2COO^-} \quad (11)$$

$$m^{total}_{R_3N} = m_{R_3N} + m_{R_3NH^+} \quad (12)$$

$$(m^{total}_{RNH_2} + m^{total}_{NH_3} + m^{total}_{R_3N}) \times \alpha = m_{RNHCOO^-} + m_{NH_2COO^-} + m_{CO_2} + m_{HCO_3^-} + m_{CO_3^{2-}} \quad (13)$$

$$m_{H^+} + m_{RNH_3^+} + m_{NH_4^+} + m_{R_3NH^+} = m_{RNHCOO^-} + m_{NH_2COO^-} + m_{HCO_3^-} + 2m_{CO_3^{2-}} + m_{OH^-} \quad (14)$$

where $m^{total}_{RNH_2}$, $m^{total}_{NH_3}$, and $m^{total}_{R_3N}$ are the initial molar concentrations of AMP, NH_3, and TEA, respectively, and α is the CO_2 loading ratio in the solvent system. Combining Eqs. (1)-(14), the partial pressure of CO_2 can be expressed as

$$P_{CO_2} = \frac{AH_{CO_2}}{\frac{K_6 m^{total}_{RNH_2}}{K_4 K_A m_{H^+}} + \frac{K_6 m^{total}_{NH_3} K_5}{K_B m_{H^+}} + \frac{K_6}{m_{H^+}} + \frac{K_6 K_3}{(m_{H^+})^2}} \quad (15)$$

$$\text{where, } A = (m^{total}_{RNH_2} + m^{total}_{NH_3} + m^{total}_{R_3N}) \times \alpha - \frac{P_{CO_2}}{H_{CO_2}} \quad (16)$$

$$K_A = 1 + \frac{m_{H^+}}{K_1} + \frac{K_6 P_{CO_2}}{K_4 H_{CO_2} m_{H^+}} \quad (17)$$

$$K_B = 1 + \frac{K_2 m_{H^+}}{K_7} + \frac{K_5 K_6 P_{CO_2}}{H_{CO_2} m_{H^+}} \quad (18)$$

The H^+ ion concentration was determined, and the pressure can be predicted from Eq. (15). The ion concentration in the blended absorbent/CO_2/H_2O system can be calculated using the equations in Table 1 and the equilibrium constant

MATERIALS AND METHODS

1. Materials

Analytical grade AMP of 99% purity was obtained from Acros Organics (USA), NH_3 (28%) was obtained from Junsei Chemical (Japan), and TEA (99%) was obtained from Sigma Aldrich (USA); distilled water was used for making the blended absorbent. The blended absorbent consisted of 20 wt% AMP, 5 wt% NH_3, 5 wt% TEA, and distilled water. The CO_2 and N_2 gases were commercial grade, of purity 99.99%, and mixed at 15 vol%.

2. Apparatus and Procedure

A schematic diagram of the apparatus is shown in Fig. 1. The experimental apparatus consisted of a gas injector, absorber, regenerator, and CO_2 analyzer. The absorber and regenerator were made of double layered glass with an internal diameter of 50 mm and a height of 600 mm. Ceramic Raschig rings (diameter 6.35 mm) were packed inside. The temperatures of the absorber and regenerator were controlled by a circulating flow of heated oil in the outside layer. The water and oil were heated at different desired temperature by oil baths. The CO_2 mixed gas was controlled by mass flow controllers (5850E, Brooks Instruments, USA), and the flow rate

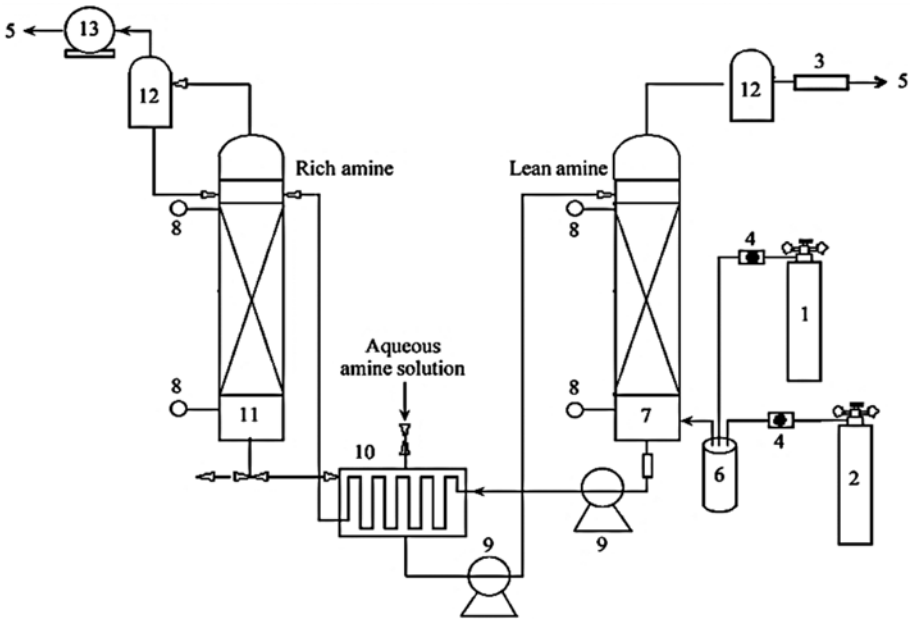

Fig. 1. Schematic diagram of experimental apparatus.

1. N_2 gas
2. CO_2 gas
3. CO_2 analyzer
4. Mass flow controller
5. Outlet
6. Mixing chamber
7. Absorber
8. Thermocouple
9. Liquid pump
10. Heat exchanger and storage tank
11. Regenerator
12. Condenser
13. Gas meter

was checked by using a gas meter (W-NK-0.5, Shinagawa, Japan). Gas chromatography (GC 7890, USA) was used to measure the CO_2 outlet gas concentration from the absorber. The condenser was connected to the top of the regenerator to prevent absorbent loss. Before the experiment, the absorber and regenerator were preheated. An aqueous amine solution was then injected into a storage tank, and the flow rate was controlled by a metering pump (Cole Parmer Masterflex Pump Model 7518-12, USA).

To study the absorption characteristics of the blended amine at various CO_2 loading ratios, experiments were performed with only the absorber operating. The absorber was heated to the desired temperature and then 500 mL of fresh or CO_2-loaded blended absorbent solution with the desired CO_2 loading ratio was injected into the storage tank. The outlet CO_2 concentration from the absorber was checked continuously using a CO_2 gas analyzer.

The experiments to investigate the effect of ion species on regeneration were carried out with both the absorber and regenerator operating. Fresh blended absorbent solution (500 mL) was injected into the storage tank and preheated. The operation began when the device reached the desired temperature; 15% CO_2 gas was injected into the bottom of the absorber, and the outlet CO_2 concentration from the absorber was measured continuously using a CO_2 gas analyzer (GC 7890). When the outlet CO_2 concentration was stable, 10 mL of lean amine solution and rich amine solution were collected for NMR analysis, pH measurements, and CO_2 loading ratio calculation. The overall experimental conditions were gas flow rate 3.5 L/min, absorbent flow rate 40 mL/min, absorber temperature 313 K, and regenerator temperature 353-383 K. The CO_2 loading ratio was analyzed by a titrimetric method [1].

3. NMR Spectroscopy

The ^{13}C NMR spectra of the absorbed or regenerated absorbents were obtained using a 500 MHz superconducting Fourier-transform NMR spectrometer (Unity-Inova 500, USA). The MestrReC software developed by MestreLab Research was used to process the spectra. The absorbent samples were diluted to (10%) by using deuterium oxide (Aldrich) to provide a sufficiently strong signal for deuterium lock. Barzagli showed that quantitative analyses could be performed by relating the area integral of the species peaks to that of the signal of a standard at known concentration [13]. In this study, the -CH_2OH carbon atoms from TEA were used as the reference, because -CH_2OH was a stable compound in solution before and after CO_2 absorption. Their known concentration in the solution was 1.0 mol/kg. All the molar concentrations of the observable species were calculated as follows [33]:

$$C_i = \frac{A_i \times \varphi_{ref} \times C_{ref}}{\varphi_i \times A_{ref}} \tag{19}$$

where C_i is the concentration of ions, A_i and A_{ref} are the experimental integrated peak area for species i and reference species (-CH_2OH carbon atoms from TEA), φ_{ref} and φ_i are the number of active carbons in reference species and species i.

RESULTS AND DISCUSSION

1. Prediction of CO_2 Partial Pressure in Blended Absorbent Solution

The apparent equilibrium constant, K_5, for the main amine reaction, Eq. (5), was assumed to be dependent on the temperature (T) and CO_2 loading (α). A least-squares fit was applied to the equilibrium solubility values obtained for CO_2 in the blended absorbent. The carbamate formation constant, K_5, was determined to give the following expression;

$$\ln K_5 = 20.15214 - \frac{604.1164}{T} - 4.017263 \ln T - 0.503095 \times 10^{-2} T - 2.27516\alpha + 3.34403\alpha^2 \tag{20}$$

The constant in Eq. (20) was regressed from the experimental solubility results for CO_2 in a blended absorbent obtained by Kang et al. [6]. The regression of carbamate formation constant is a fundamental and important effect because of the crucial role played by the carbamate formation reaction in the CO_2 absorption system. It can be used for the determining or modeling the ions behaviors in the CO_2 absorption process. These data points pertain to the blended absorbent at 313, 353, 363, 373, and 383 K. The CO_2 partial pressure can be predicted using Eq. (15); the results are shown in Fig.

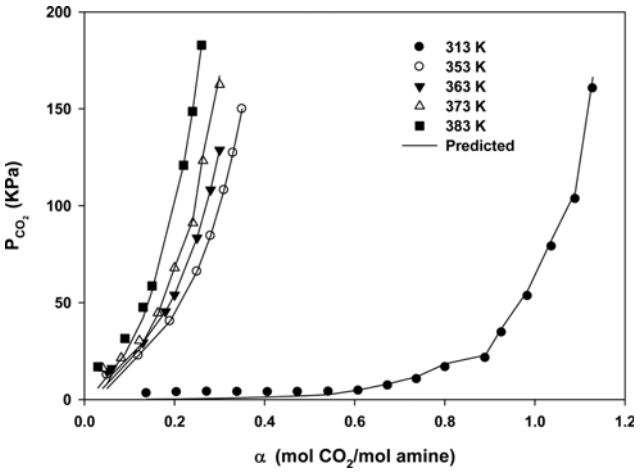

Fig. 2. Plot of pressure against α, illustrating the solubility of CO_2 in blended absorbent at various temperatures. Data from [6]; smoothed lines: modified Kent-Eisenberg model calculation.

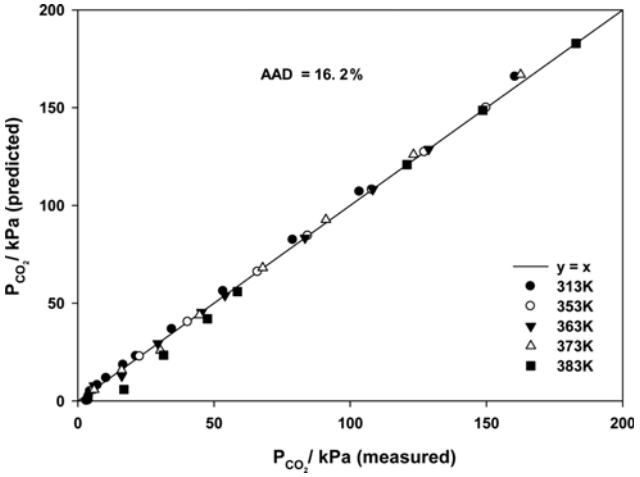

Fig. 3. Plot of predicted partial pressures (calculated using the modified Kent-Eisenberg model) against measured partial pressures for CO_2 in blended absorbent.

2, and the satisfactory results are shown in Fig. 3, which contains a plot comparing the predicted and measured partial pressures of CO_2 in the blended absorbent. The average absolute deviation (AAD) between experimental data and the predication data was 16.2%. As Fig. 3 suggests, the applied model well-represented the solubility of CO_2 in the blended absorbent at the experimental conditions studied.

2. Absorption of CO_2 by Blended Absorbent

^{13}C NMR spectroscopy was performed on the blended amine/CO_2/H_2O system (before CO_2 loading and after), as shown in Fig. 4 and Table 2. Peaks forming AMP/$AMPH^+$, TEA/$TEAH^+$, carbamate, and HCO_3^-/CO_3^{2-} were identified. Carboxyl groups from carbamate, and bicarbonate and carbonate were observed downfield ($166<\delta<160$ ppm) in the spectra. Because AMP-COO^- and NH_2COO^- had the same carboxyl groups, they appeared at the same position (δ=165.54 ppm). As reported in the literature [38,39], as a result of fast proton exchange, it is not possible to distinguish between HCO_3^- and CO_3^{2-}, and the HCO_3^- and CO_3^{2-} ions appear as a single peak (δ=162.72 ppm). Holmes developed a method for calculating the concentrations of carbonate and bicarbonate in $NH_3/H_2O/CO_2$ systems, but it is not applicable to mixed amine systems [40]. There is no carbon in NH_3/NH_4^+ ions, so NH_3/NH_4^+ ions did not appear in the ^{13}C NMR spectra.

Fig. 5 shows a comparison of the speciation results for the blended absorbent at 313 K from the model and those from the NMR data, for AMP/$AMPH^+$, TEA/$TEAH^+$, NH_3/NH_4^+, carbamate, and HCO_3^-/CO_3^{2-}. The model predictions agree well with the experimental results. As it is difficult to experimentally distinguish between protonated and unprotonated amines, because of the fast proton exchange mechanism, only the sum of the two components can be reported. However, the modified Kent-Eisenberg model can be used to calculate the amounts of protonated and unprotonated amine ions in Fig. 5 and the predicted results were indicated by solid line. The TEA/$TEAH^+$ concentration remains almost constant and that of AMP/$AMPH^+$ decreases slightly. As the CO_2 loading increases, the $AMPH^+$ concentration increases because the solution pH decreases; the AMP concentration shows the converse trend [18]. Because of the steric hindrance of AMP, AMP-COO^- is rapidly converted to carbonate/bicarbonate [41]. The total carbamate concentration increases with increasing CO_2 loading ratio, reaches a maximum at approximately 0.6 mol CO_2/mol amine, and then subsequently shows a slight decrease. Unlike carbamate, the concentrations of carbonate and bicarbonate ions significantly increase. The carbamate ions are converted to other species such as carbonate/bicarbonate, as shown in Eqs. (4) and (5). More carbamate can be converted to bicarbonate and carbonate, enhancing the CO_2 absorption ability, under CO_2-rich conditions, so the CO_2 loading ratio should be controlled to more than 0.6 mol CO_2/mol amine. Also, by addition of AmH (in this study, NH_3 is AmH), AMP-COO^- can be completely converted to free AMP [15]. The reaction is

$$AMPH^+ + AMPCOO^- + 2AmH \rightarrow AmH_2^+ + AmCOO^- + 2AMP \quad (21)$$

Eq. (21) shows that NH_3 can enhance the conversion of AMP-COO^- to NH_2COO^-. This indicates that NH_2COO^- is the main compound in the total carbamate, as in the predicted results.

In Fig. 6, experimental speciation results at the regeneration temperature (373 K) were presented as plots, and the model predictions were presented as solid lines. At low CO_2 loading ratios, the carbamate concentration was greater than that of HCO_3^-/CO_3^{2-}. It is known that at high temperature, carbamates are more stable than bicarbonate. The bicarbonate formed was therefore unstable, which is favorable for regeneration [42]. Carbonyl group species such as

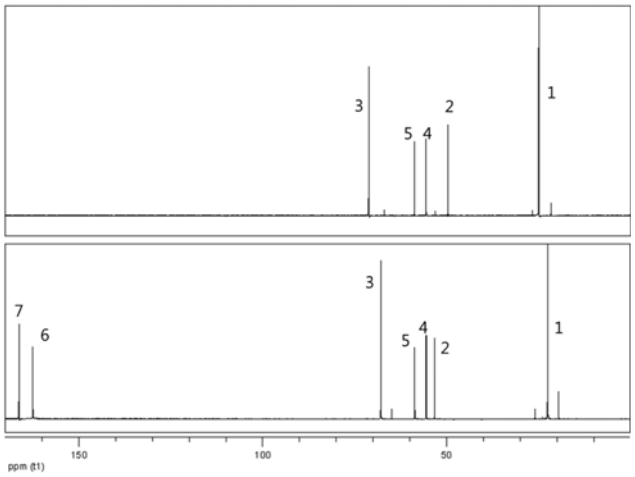

Fig. 4. ^{13}C NMR spectra of blended absorbent solution (a: fresh absorbent; b: CO_2-loaded absorbent, 0.41 mol CO_2/mol amine).

Table 2. Assignments of observed bands in CO_2-loading blended absorbents in Fig. 3(b)

No.	Carbon atoms	AMP/ $AMPH^+$	TEA/ $TEAH^+$	HCO_3^-/ CO_3^{2-}	AMP-COO^-/ NH_2COO^-
1	-CH_3	22.53	-	-	-
2	-C-NH_2	49.76	-	-	-
3	-CH_2OH	67.09	-	-	-
4	-N-CH_2-	-	55.54	-	-
5	-CH_2OH	-	58.86	-	-
6	-HCO_3^-/CO_3^{2-}	-	-	162.72	-
7	-N-COO^-	-	-	-	165.54

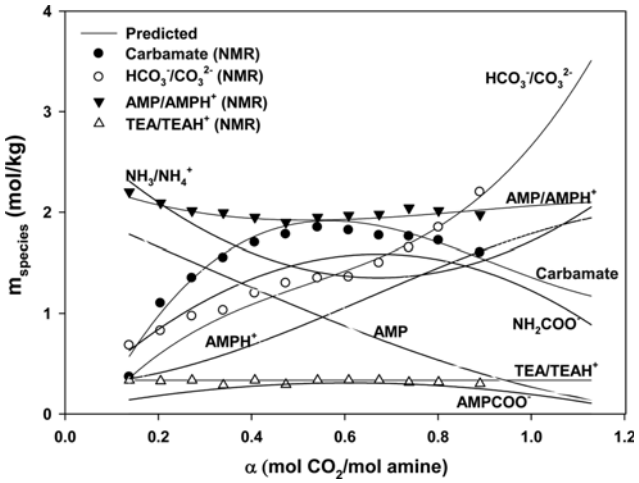

Fig. 5. Ion species concentrations in CO_2-loaded blended absorbent, obtained using ^{13}C NMR quantitative analysis, with respect to various CO_2 loading ratios, at 313 K.

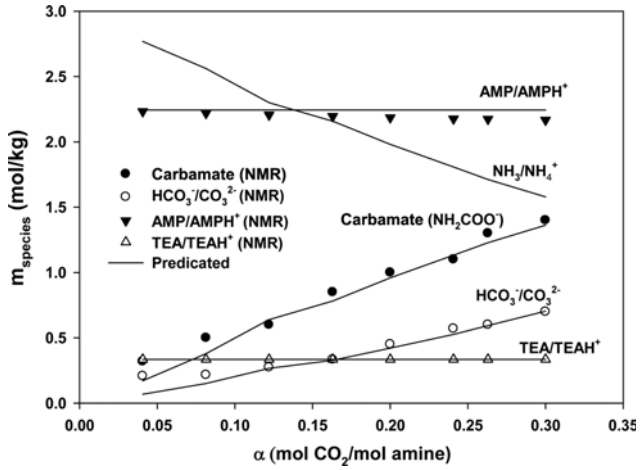

Fig. 6. Ions species concentrations in CO_2-loaded blended absorbent, obtained using ^{13}C NMR quantitative analysis, with respect to various CO_2 loading ratios, at 373 K.

carbamate, carbonate, and bicarbonate are important factors in the CO_2 capture process. Figs. 5 and 6 show the trends in the relative concentrations of carbonyl group species at equilibrium in the liquid phase, as functions of temperature and CO_2 loading. Once the CO_2 loading ratio is known, the carbonyl group species concentration can be predicted. In the absorption and regeneration processes, since the CO_2 loading ratio can be directly measured by titrimetrical method, it is easy to predict the carbonyl group species.

To study the effect of CO_2 loading ratio on the CO_2 removal efficiency, the absorber was operated without the regenerator, with a CO_2-loaded blended absorbent. Fig. 7 shows the effects of the CO_2 loading ratio of the blended absorbent and species distribution on the CO_2 removal efficiency. The removal efficiency remains high at low CO_2 loading ratios, and decreases with increasing CO_2 loading. Arashi et al. [43] reported that if the CO_2 loading in a lean solution was high, the driving force of mass transfer from the gas to solution became small, and the CO_2 removal efficiency decreased. In addition, when the carbamate concentration was much greater than that of HCO_3^-/CO_3^{2-} ions, the CO_2 absorption efficiency decreased sharply.

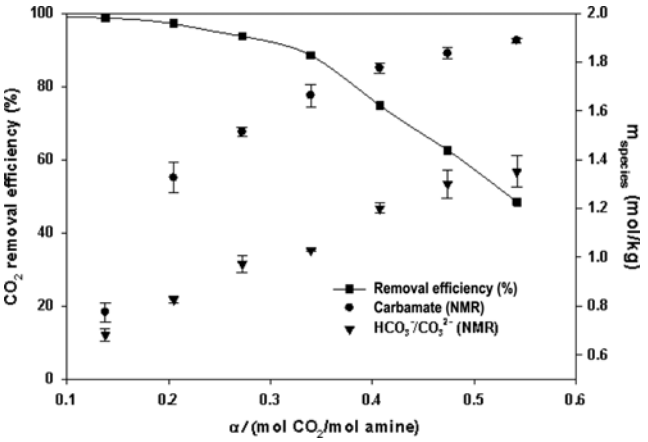

Fig. 7. CO_2 removal efficiency and concentration of species in CO_2-loaded blended absorbent with respect to various CO_2 loading ratios.

The results confirm that carbamate formation negatively affects the CO_2 absorption efficiency. As HCO_3^- inhibits the CO_2 hydration rate in the liquid phase, as shown in Eq. (6), the concentration of HCO_3^- in the regeneration step should be reduced, resulting in higher CO_2 conversion in the absorber [44]. The CO_2 loading should be less than 0.3 mol CO_2/mol amine to maintain CO_2 removal efficiency greater than 90%.

3. Absorption and Regeneration Test for Blended Absorbent

3-1. Characteristics of Absorption and Regeneration, Depending on Regenerator Temperature

Continuous absorption and regeneration experiments were carried out to study the regeneration characteristics of the blended absorbent. The operating conditions and method are described in section 3.2; rich- and lean-amine samples were picked at the steady-state, and the CO_2 loading ratio and concentration of carbonyl group species were analyzed (the analysis methods are described in sections 3.2 and 3.3).

Fig. 8 shows the CO_2 stripping efficiency with respect to regeneration temperature. The CO_2 stripping efficiency can be calculated from the CO_2 loading ratios under CO_2-rich and CO_2-lean conditions [45]. The amount of CO_2 loaded in the blended absorbent depends specifically on the carbonyl group species. CO_2 is mainly stored in the blended absorbent as HCO_3^-/CO_3^{2-} and carbamate. For HCO_3^-/CO_3^{2-} ions, the concentration of ions after regeneration decreased significantly; the decrease in HCO_3^-/CO_3^{2-} at 353 K was 0.20 mol/kg, and it reached 1.59 mol/kg at 383 K. In contrast, the concentration of carbamate increased slightly up to 363 K and then decreased at 373 K. This indicates that with increasing temperature, some HCO_3^-/CO_3^{2-} was compensated for by an increase in carbamate. The decreases in HCO_3^-/CO_3^{2-} with a lean amine at various regeneration temperatures were greater than those of carbamate, and the amounts of bicarbonate and carbonate ions decreased more than that of carbamate. The results show that the regeneration of CO_2 mainly originates from HCO_3^-/CO_3^{2-} species. Carbamate has a negative effect on CO_2 regeneration [10]. This can be interpreted based on the regeneration mechanism of the blended absorbent. According to previous reports, bicarbonate is relatively easily decomposed

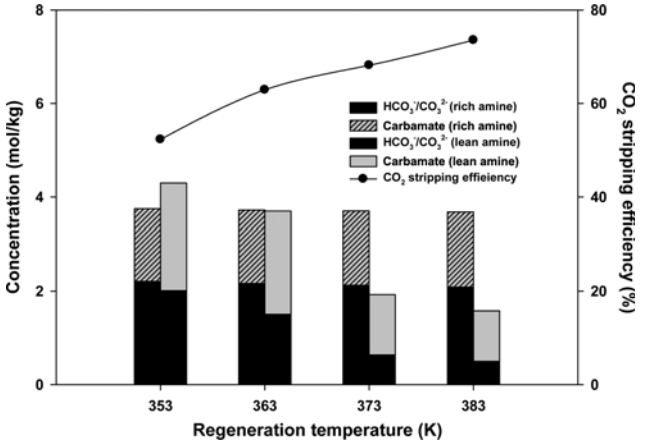

Fig. 8. CO_2 stripping efficiency and concentration of carbonyl group species in CO_2-loaded blended absorbent with respect to regeneration temperature. Bars in the left- and right-hand sides are for blended absorbent before and after regeneration, respectively.

by heating and is expected to decompose at a significant rate at temperatures above 333 K [46]. In addition, during the regeneration step, breaking of the less-stable C-O bonds in bicarbonate and carbonate requires less energy than that required to break the C-N bonds in carbamate species [46]. The primary goal of the regeneration process in CO_2 capture is to maximize regeneration of the blended absorbent, in order to maintain a high loading capacity and absorption efficiency. In addition, to reduce the negative effect of carbamate on CO_2 stripping, the regeneration temperature was fixed at 373 K in the following experiments. However, unlike the $NH_3/CO_2/H_2O$ system, ammonium carbamate can be released up to 333 K, so the regeneration temperature was less in this study. Because AMP and TEA have higher specific heats than NH_3, a blend of AMP and TEA may cause more regeneration heat and the regeneration temperature should be higher than that of NH_3 [47,48].

3-2. Behaviors of Carbonyl Group Species with Respect to Operating Time

Investigation of carbonyl group ion behavior in continuous absorption and regeneration processes is important as these groups can be used for retaining CO_2. Quantitative ^{13}C NMR spectroscopy can be used to calculate the concentrations of carbonyl group species. The continuous absorption and generation experiments discussed in this section were performed as described in section 3.2. Fig. 9 shows the concentrations of carbonyl group ions measured using NMR spectroscopy and predicted from the CO_2 loading ratio. As expected, the carbonyl group species attained equilibrium after 90 min. At the start of the experiment, in the absorbent, carbamate formation stabilized more quickly than carbonate and bicarbonate formation. This indicates that the carbamate formation rate was higher than that of bicarbonate [46,48]. The blended absorbent has an excellent absorption ability and absorption rate [6], so species formation quickly stabilizes. In addition, carbamate formation and bicarbonate formation occur at the same time. According to research, some of the carbamate is converted to bicarbonate, causing the concentrations of bicarbonate and carbonate species to increase compared with that of carbamate. Up to 20 min, the blended absorbent was fresh, a large amount of free amines was present, and the concentration of carbamate was increasing. However, after 20 min, the absorber started to become rich in CO_2, enhancing bicarbonate conversion. For a lean amine in the regenerator, the change in the carbamate concentration with operating time was not significant, and it was not easy to deposit carbamate ions. We compared the carbonyl group species concentration before and after regeneration; the reduction in bicarbonate species concentration was greater than the reduction in carbamate concentration. This depended greatly on the species structure [42]. As carbonyl species affect the CO_2 stripping efficiency, the concentration of carbonyl species in the rich amine was 5.39 mol/kg while the concentration in the lean amine was 2.08 mol/kg. Especially, 3.31 mol/kg of carbon can be stripped from the blended absorbent in one cycle of the continuous absorption and regeneration process. In addition, the regeneration efficiency was 73.86%, calculated from the CO_2 loading ratio in the rich and lean amines.

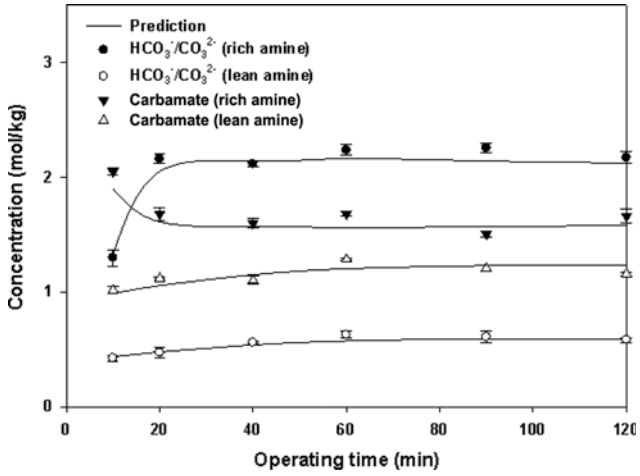

Fig. 9. Effect of absorption and regeneration process operating time on carbonyl group species behaviors in lean-amine and rich-amine solutions.

Table 3 shows the carbonyl species predicted from the model equations and the CO_2 loading ratios. The CO_2 loading ratio samples were picked from the absorber and regenerator at 10, 20, 40, 60, 80, and 120 min, and the ratios were determined using a titrimetric method. The AAD% values show that the predicted results were close to the experimental results obtained using NMR spectroscopy. These methods can be applied to CO_2 absorption and regeneration processes with a blended absorbent.

CONCLUSION

Speciation in a blended absorbent/CO_2/H_2O system was determined using ^{13}C NMR spectroscopy, and predicted using a modified Kent-Eisenberg model. The predicted results were in agreement with

Table 3. Comparison of NMR spectroscopic results and predicted results

Time (min)	CO_2 loading ratio (rich amine)	CO_2 loading ratio (lean amine)	NMR	Prediction	NMR	Prediction	NMR	Prediction	NMR	Prediction
			HCO_3^-/CO_3^{2-} (rich amine)		Carbamate (rich amine)		HCO_3^-/CO_3^{2-} (lean amine)		Carbamate (lean amine)	
10	0.55	0.21	1.30	1.33	1.90	2.05	0.43	0.42	0.99	1.02
20	0.87	0.22	2.16	2.05	1.61	1.68	0.48	0.47	1.06	1.12
40	0.90	0.24	2.11	2.14	1.57	1.60	0.54	0.56	1.15	1.10
60	0.92	0.26	2.23	2.17	1.56	1.68	0.57	0.63	1.20	1.28
90	0.90	0.26	2.25	2.14	1.57	1.50	0.59	0.61	1.23	1.20
120	0.90	0.26	2.17	2.12	1.58	1.66	0.59	0.58	1.23	1.16
AAD%	-		3.16		5.17		3.56		4.62	

the experimental data. The carbamate formation constant was regressed as a function of temperature and CO_2 loading ratio, and the equation was $\ln K_5 = 20.15214 - (604.1164/T) - 4.017263 \ln T - 0.503095 \times 10^{-2} T - 2.27516\alpha + 3.34403\alpha^2$. The carbamate equilibrium constant is indispensable for determining and modeling the vapor-liquid equilibria in the CO_2 absorption process and the calculation of the carbamate formation. ^{13}C NMR qualitative analysis was used to identify the AMP/$AMPH^+$, TEA/$TEAH^+$, carbamate, and HCO_3^-/CO_3^{2-} species peaks. The speciation results showed that carbamate had a peak at a certain CO_2 loading ratio (nearly 0.6 mol CO_2/mol amine), and was converted to bicarbonate; the HCO_3^-/CO_3^{2-} concentration increased with increasing CO_2 loading ratio. In absorption experiments, the carbamate concentration limited the absorption efficiency, and the CO_2 loading ratio needed to be below 0.3 mol CO_2/mol amine to maintain the CO_2 removal efficiency above 90%.

Investigation of the effects of carbonyl group species behavior in absorption and regeneration experiments showed that carbamate ions have a negative effect on regeneration in a range of low regeneration temperatures, and HCO_3^-/CO_3^{2-} has a positive effect. The best regeneration temperature in terms of energy reduction and maximum absorption ability in the CO_2 capture process was 373 K. The results showed that prediction equations and NMR analysis could provide an easy way to determine the carbonyl group species concentration. This will be helpful in optimizing CO_2 capture processes using blended absorbents.

ACKNOWLEDGEMENTS

This work was supported by the first stage of Brain Korea 21 Plus Project in 2013 and the Korea Institute of Energy Technology Evaluation and Planning (KETEP), granted financial resource from the Ministry of Trade, Industry & Energy, Republic of Korea (No. 20102010200006B-13-1-000).

NOMENCLATURE

α : CO_2 loading ratio
φ_i : the number of active carbons in species i
φ_{ref} : the number of active carbons in reference species
A_i : the experimental integrated peak area for species i
C_i : the concentration of ions
K_i : the equilibrium constant
R_b : the number of moles of reference/kg solution per unit area
T : absolute temperature
$m_{species}$: molarity of species in absorbent solution
AMP : 2-amino-2-methylpropranol
DEA : diethanolamine
TEA : triethanolamine
MDEA : methyldiethanolamine
MEA : monoethanolamine
NMR: nuclear magnetic resonance
VLE : vapor-liquid equilibrium

REFERENCE

1. W. J. Choi, B. M. Min, B. H. Shon, J. B. Seo and K. J. Oh, *J. Ind. Eng. Chem.*, **15**, 635 (2009).
2. P. Zhang, Y. Shi, J. Wei, W. Zhao and Y. Qing, *J. Environ. Sci.*, **20**, 39 (2007).
3. W. J. Choi, B. M. Min, J. B. Seo, S. W. Park and K. J. Oh, *Ind. Eng. Chem. Res.*, **48**, 4022 (2009).
4. J. K. You, H. S. Park, S. H. Yang, W. H. Hong, W. Shin, J. K. Kang, K. B. Yi and J. N. Kim, *J. Phys. Chem. B*, **112**, 4323 (2008).
5. J. B. Seo, S. B. Jeon, J. Y. Kim, G. W. Lee, J. H. Jung and K. J. Oh, *J. Environ. Sci.*, **24**, 494 (2012).
6. M. K. Kang, S. B. Jeon, M. H. Lee and W. J. Oh, *Korean J. Chem. Eng.*, **30**, 1171 (2013).
7. L. S. Tan, A. M. Shariff, K. K. Lau and M. A. Bustam, *J. Ind. Eng. Chem.*, **18**, 1874 (2012).
8. C. K. Anh, H. W. Lee, Y. S. Chang, K. W. Han, J. Y. Kim, C. H. Rhee, H. D. Chun, M. W. Lee and J. M. Park, *Int. J. Greenhouse Gas Control*, **5**, 1606 (2011).
9. I. Masaki, E. Takahiko and S. Daisuke, *Mitsubishi Heavy Industries Technical Review*, **47**, 37 (2010).
10. M. Nitta, M. Hirose, T. Abe, Y. Furukawa, H. Sato and Y. Yamanaka, *Energy Procedia*, **37**, 869 (2013).
11. Q. Yang, M. Bown, A. Ali, D. Winkler, G. Puxty and M. Attalla, *Energy Procedia*, **1**, 955 (2009).
12. J. P. Jakobsen, J. Krane and H. F. Svendsen, *Ind. Eng. Chem. Res.*, **44**, 9894 (2005).
13. F. Barzagli, F. Mani and M. Peruzzini, *Energy Environ. Sci.*, **2**, 322 (2009).
14. A. F. Ciftja, H. Ardi, E. F. Silva and H. F. Svendsen, *Energy Procedia*, **4**, 614 (2011).
15. B. Francesco, M. Fabrizio and P. Maurizio, *Int. J. Greenhouse Gas Control*, **16**, 217 (2013).
16. C. K. Ahn, H. W. Lee, Y. S. Chang, K. Han, J. Y. Kim and C. H. Rhee, *Int. J. Greenhouse Gas Control*, **5**, 1606 (2011).
17. C. K. Ahn, H. W. Lee, M. W. Lee, Y. S. Chang, K. R. Han, C. H. Rhee, J. Y. Kim, H. D. Chun and J. M. Park, *Energy Procedia*, **4**, 541 (2011).
18. D. Tong, J. P. Trusler, G. C. Maitland, J. Gibbins and P. S. Fennell, *Int. J. Greenhouse Gas Control*, **6**, 37 (2012).
19. F. Barzaglia, F. Mania and M. Peruzzinib, *Int. J. Greenhouse Gas Control*, **5**, 448 (2011).
20. M. Ballard, M. Bown, S. James and Q. Yang, *Energy Procedia*, **4**, 291 (2011).
21. F. Barzagli, F. Mani and M. Peruzzini, *Energy Environ. Sci.*, **3**, 772 (2010).
22. R. J. Hook, *Ind. Eng. Chem. Res.*, **36**, 1779 (1997).
23. C. C. Chen and L. B. A. Evans, *AIChE J.*, **32**, 444 (1986).
24. R. D. Deshmukh and A. E. Mather, *Chem. Eng. Sci.*, **36**, 355 (1981).
25. R. L. Kent and B. Eisenberg, *Hydrocarbon Process.*, **55**(2), 87 (1976).
26. W. A. Fouad and A. S. Berrouk, *Ind. Eng. Chem. Res.*, **51**, 6591 (2012).
27. P. Tontlwachwuthlkul, A. Meisen and C. J. Lim, *J. Chem. Eng. Data*, **36**, 130 (1991).
28. M. D. Cheng, A. R. Caparanga, A. N. Soriano and M. H. Li, *J. Chem. Thermodyn.*, **42**, 342 (2010).
29. S. Guldo and W. S. David, *Ind. Eng. Chem. Fundam.*, **22**, 239 (1983).
30. D. H. Lee, W. J. Choi, S. J. Moon, S. H. Ha, I. G. Kim and K. J. Oh, *Korean J. Chem. Eng.*, **25**, 279 (2008).
31. G. Mahdi, T. Vahid, G. Cirous, A. A. Safekordi and N. Hesam, *Iran.*

J. Chem. Chem. Eng., **29**, 111 (2010).
32. K. Kawasuishi and J. M. Prausnitz, *Ind. Eng. Chem. Res.*, **26**, 1482 (1987).
33. A. F. Ciftja, A. Hartono and H. F. Svendsen, *Int. J. Greenhouse Gas Control*, **16**, 227 (2013).
34. W. A. Fouad and A. S. Berrouk, *Ind. Eng. Chem. Res.*, **51**, 6591 (2012).
35. S. H. Park, S. H. Kim and B. M. Min, *J. Korean Ind. Eng. Chem.*, **9**, 107 (1998).
36. T. J. Edwards, J. Newman and J. M. Prausnitz, *Am. Inst. Chem. Eng.*, **21**, 248 (1975).
37. B. Rumpf and G. Maurer, *Ind. Eng. Chem. Res.*, **32**, 1780 (1993).
38. J. S. Morrow, P. Keim and F. R. N. Gurd, *J. Biol. Chem.*, **249**, 7484 (1974).
39. J. L. Zweier, J. B. Wooten and J. S. Cohen, *Biochemistry*, **20**, 3505 (1981).
40. P. E. Holmes II, M. Naaz and B. E. Poling, *Ind. Eng. Chem. Res.*, **27**, 3281 (1998).
41. J. H. Choi, S. G. Oh, Y. Yoon, S. K. Jeong, K. R. Jang and S. C. Nam, *J. Ind. Eng. Chem.*, **18**, 568 (2012).
42. Y. E. Kim, J. A. Lim, S. K. Jeong, Y. Yoon, S. T. Bae and S. C. Nam, *Bull. Korean Chem. Soc.*, **34**, 783 (2013).
43. N. Arashi, N. Oda, M. Yamad, H. Ota, S. Umeda and M. Tajika, *Energy Convers. Manage.*, **38**, 63 (1997).
44. I. Iliuta and F. Larachi, *Sep. Purif. Technol.*, **86**, 199 (2012).
45. F. Bougie and M. C. Iliuta, *Chem. Eng. Sci.*, **65**, 4746 (2010).
46. D. Y. Kim, H. M. Lee, S. K. Min, Y. Cho, I. C. Hwang, K. Han, J. Y. Kim and K. S. Kim, *J. Phys. Chem. Lett.*, **2**, 689 (2011).
47. S. C. Ho, J. M. Chen and M. H. Li, *J. Chin. Inst. Chem. Eng*, **38**, 349 (2007).
48. J. Z. Liu, S. J. Wang, H. F. Svendsen, M. U. Idrees, I. Kim and C. H. Chen, *Int. J. Greenhouse Gas Control*, **9**, 148 (2012).
49. W. B. Budzianowskl, *Environ. Protect. Eng.*, **37**, 5 (2011).